Evaluation of Deep Learning-Synthesized Pediatric CT scans for Use in Transcranial Focused Ultrasound Treatment Planning

Julian Papasodaro[1], George M. Ibrahim[1, 2], Adam C Waspe[1, 3]

1. Neuroscience and Mental Health, The Hospital for Sick Children, Toronto, ON, Canada
2. Institute of Biomedical Engineering (BME), University of Toronto, Toronto, ON, Canada
3. Department of Material Science and Engineering, University of Toronto, Toronto, ON, Canada

Questions or comments? Please email me at julian.papasodaro@mail.utoronto.ca

At-a-glance:

Deep learning-synthesized CT scans generated from MR may enable a radiation-free treatment planning solution for pediatric transcranial focused ultrasound therapies.

Introduction

- Transcranial focused ultrasound (tFUS) is gaining traction as a therapeutic intervention for treating oncological, neurological and movement disorders in pediatric populations [1].
- Computed tomography (CT) scans are used to estimate acoustic skull properties and are required for pre-treatment simulation and planning [2].
- Exposure to ionizing radiation during CT scans presents a particular risk to children because of their larger window of opportunity for expressing radiation damage and their elevated radiation sensitivity. [3]
- There is an unmet clinical need to eliminate CT scanning from pediatric tFUS.

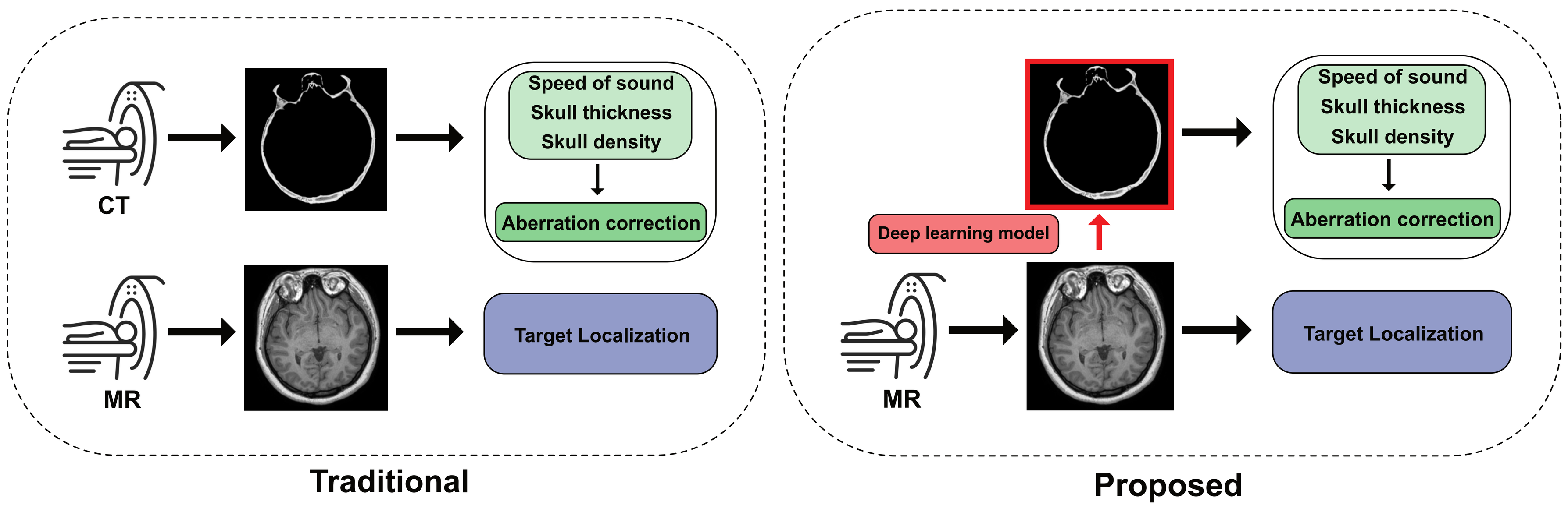

Figure 1. Illustration of traditional and proposed pre-treatment imaging methodologies for tFUS procedures.

Objective

To use deep learning to generate synthetic CT (sCT) scans capable of replacing real CT (rCT) scans in the pre-treatment planning of pediatric tFUS procedures.

Methods

Image acquisition and processing

- A pediatric trauma imaging database at the Hospital for Sick Children was retrospectively searched for paired T1-weighted and CT scans in patients aged 5-18 with no severe cranial abnormalities.
- Data from 21 patients were used with a training/validation/testing split of 10/5/6.
- MR images were acquired on either a 3T Siemens Skyra system or a 3T Philips Achieva system.
- CT images were acquired on either a GE Discovery system or a GE Revolution system.
- Paired images were resampled to a common resolution and rigidly registered using 3D Slicer.
- Non-skull features in the CT image were filtered using a 400 HU threshold filter, and high-intensity voxels were clipped to a value of 1650 HU.

Deep learning framework and training

- We employed a U-Net architecture - a convolutional neural network architecture widely used in medical imaging (Figure 2).
- The input to the network was the pre-processed MR image and the ground truth was the pre-processed CT image.
- The model was trained for 500 epochs with a mean squared error loss function and the Adam optimizer with an initial learning rate of 1e-4.

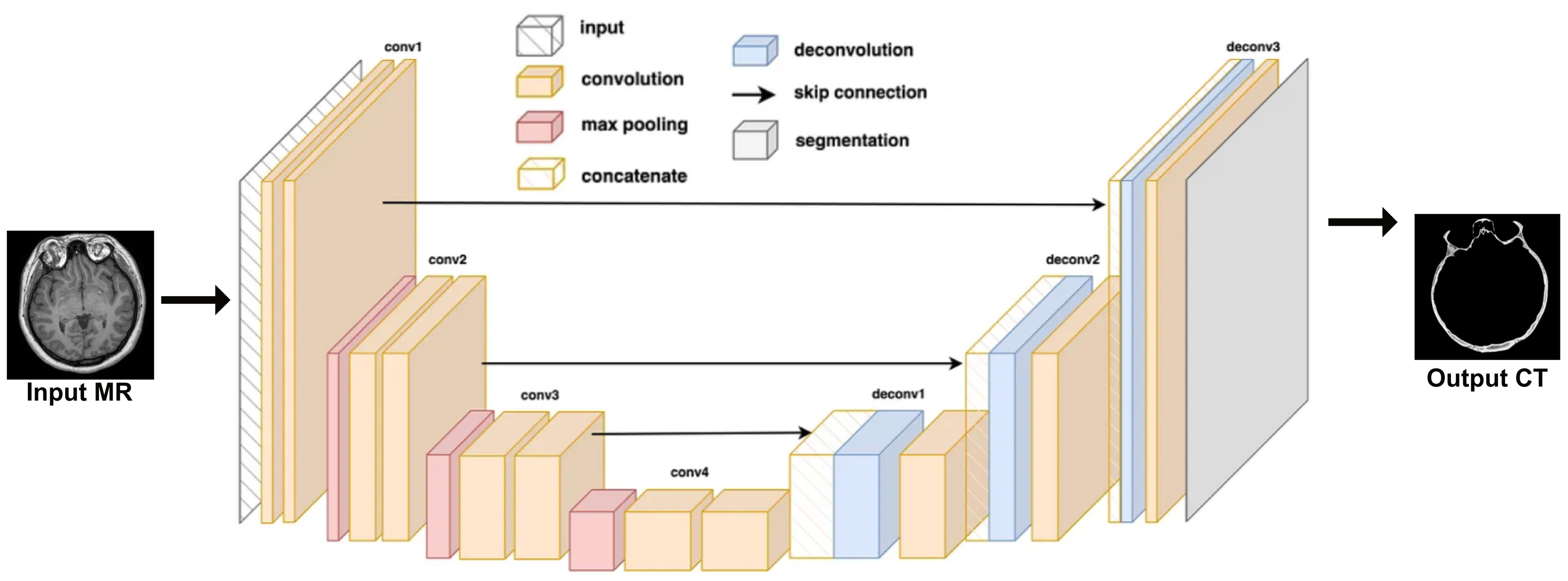

Figure 2. U-Net architecture used for generating sCT images.

Skull metric comparison

- Co-registered CT and MR images were loaded into Kranion, an interactive tFUS visualization and planning software that uses a ray-tracing algorithm to compute acoustic properties.
- Acoustic properties of the skull and treatment parameters - number of active elements (NAE); skull density ratio (SDR); skull thickness (ST) - were calculated for each virtual ray emitted from Insightec's ExAblate phased-array transducer system
- The ExAblate system was used to target the hypothalamus, left thalamus, and right thalamus.

Acoustic simulation

- Transducer geometry, acoustic properties, and the CT volume were exported from Kranion.
- Acoustic simulations were performed in kWave using the aforementioned transducer and anatomical targets.
- The operating transducer frequency was set to 650 kHz and each transducer element magnitude was set to 0.1 MPa.
- The skull was incorporated in simulation using a linear approximation to map HU to bone porosity and porosity to speed of sound, density, and absorption.

Results

Image fidelity metrics

- Qualitatively, we observed that the sCT images matched the rCT images geometrically in the calvarium but failed to replicate the fine-grain resolution at the skull base.
- Qualitatively, we observed a mean average error of 456.95 ± 44.2 HU, a dice similarity coefficient of 0.76 ± 0.05, and a structural similarity index measure of 0.91 ± 0.01 in the skull.

Results

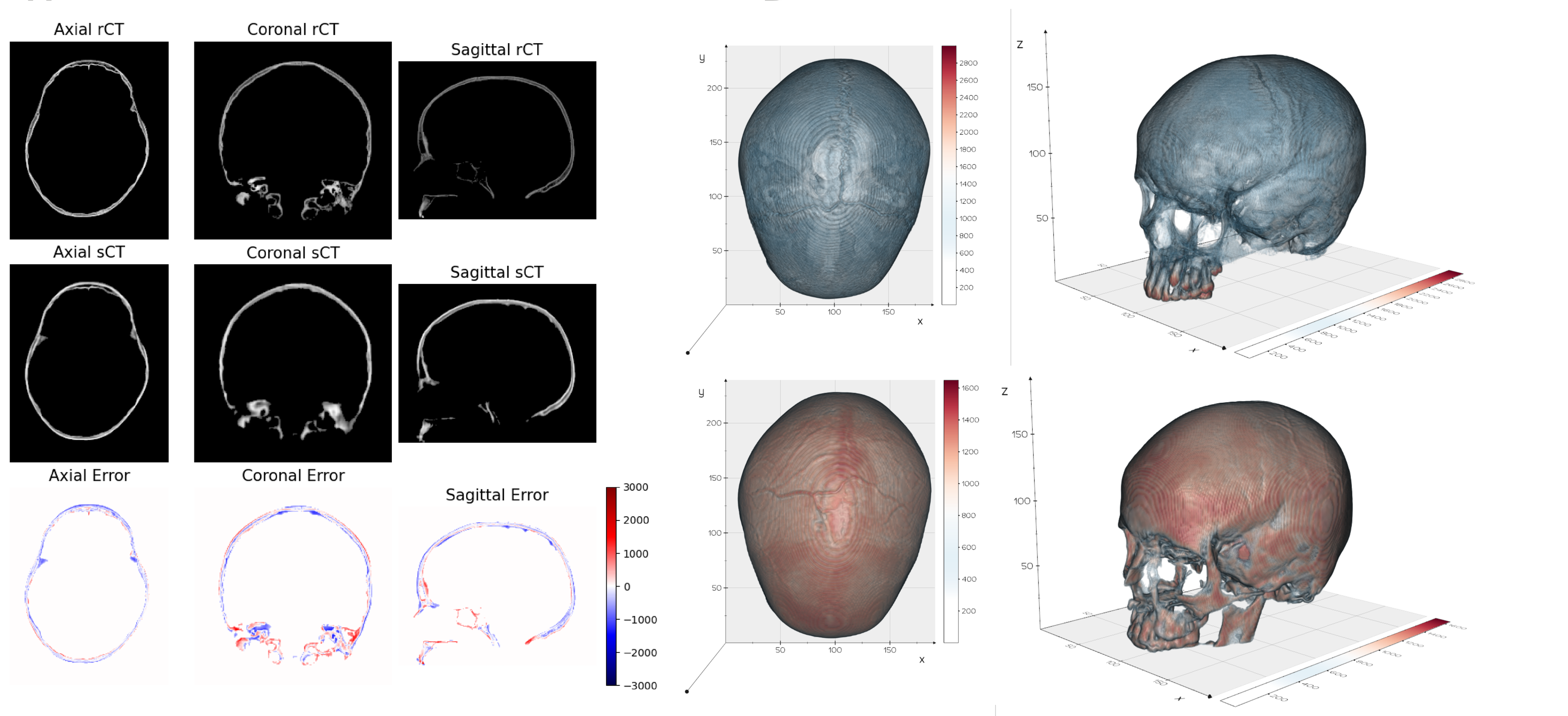

Figure 3: 2D slices of rCT, sCT and pixelwise error (A) and 3D birds-eye-view and isometric renderings of rCT (top) and sCT (bottom).

Skull metrics

- We observed that skull metrics from Kranion exhibited a moderate similarity between sCT and rCT across the evaluated targets. Trend lines from Figure 4 suggest that the SDR is overestimated in sCT.
- The Pearson's correlation coefficients for the NAE, SDR, and ST were 0.886, 0.786, and 0.759 ($p < 0.001$ in all cases). *P*-values from the Wilcoxon signed rank test found a difference between rCT- and sCT-derived SDR (p = 7.63e-6) but no differences between NAE (p = 0.304) or ST (p = 0.167).
- The mean differences between rCT and sCT were 1.92 ± 1.48%, 19.7 ± 5.11%, and 6.89 ± 3.61% for NAE, SDR, and ST, respectively.

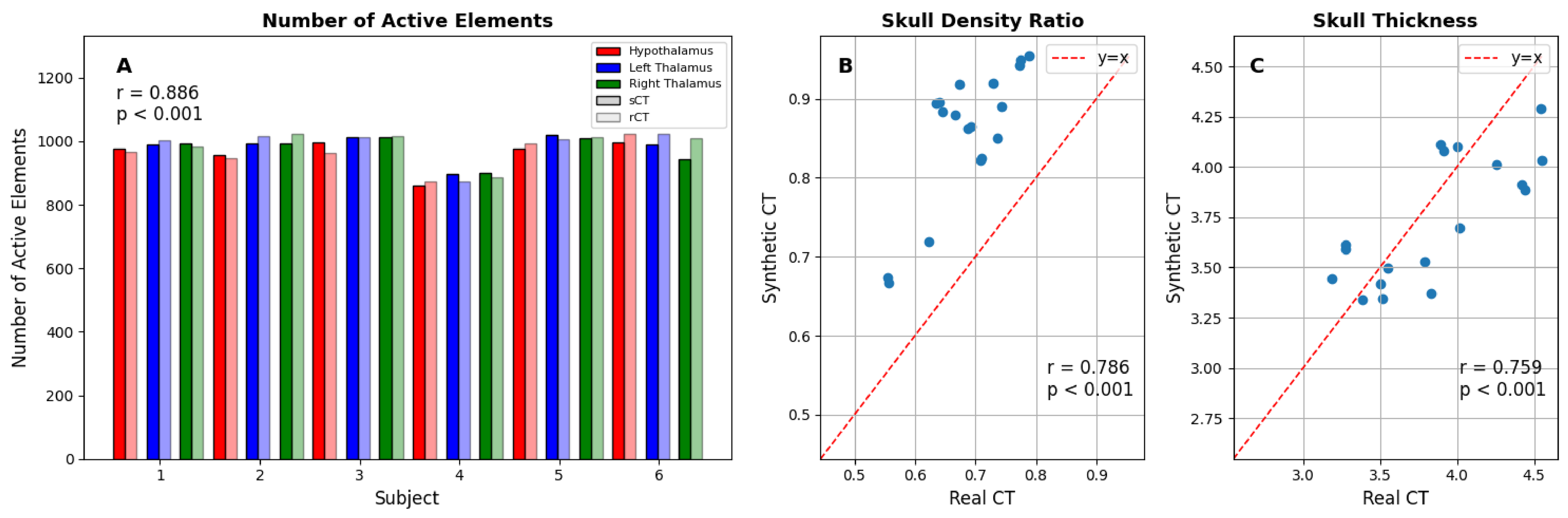

Figure 4: Kranion-derived tFUS metrics - number of active elements (A), skull density ratio (B), and skull thickness (C).

Acoustic simulation

- Acoustic simulations from using rCT and sCT data from one patient yielded pressure fields of similar geometry (Figure 5).
- The distance between the locations of peak pressure in the rCT and sCT was 1.83 mm.
- The rCT peak pressure was 1.05 MPa whereas the sCT peak pressure was 0.45 MPa.

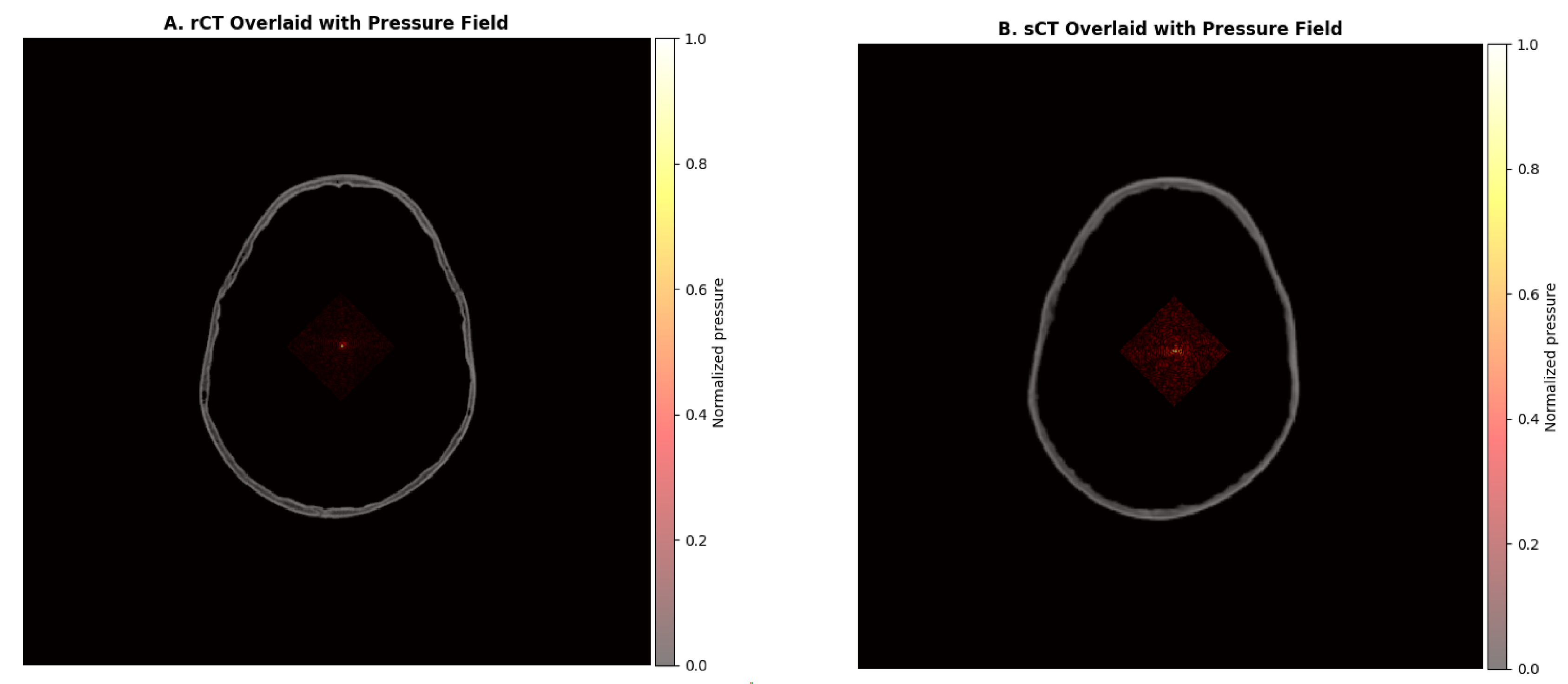

Figure 5: Axial slices of pressure field overlaid with CT scans.

Conclusions

- Deep-learning generated sCT does not generate sCT volumes from T1-weighted scans accurately enough to replace rCT scans in pre-treatment planning.
- In particular, the sCT volumes consistently overestimate the SDR which causes error when predicting the peak acoustic pressure.
- The lack of statistical difference found between rCT- and sCT-derived NAE and ST suggests that the model predicts the skull geometry with high accuracy, which may explain the small distance in peak pressure locations.
- Future work will be done to crop MR and CT volumes to exclude regions that are unimportant for tFUS planning; enlarge the data set and ensure balanced age and MR-vendor distributions;

References

[1] National Cancer Institute, "Radiation Risks and Pediatric Computed Tomography," National Cancer Institute, Sep. 04, 2018. https://www.cancer.gov/about-cancer/causes-prevention/risk/radiation/pediatric-ct-scans.

[2] M. Wang, Z. Xu, and B. Cheng, "Systematic review of phase aberration correction algorithms for transcranial focused ultrasound," iRADIOLOGY, vol. 3, no. 26–46, Dec. 2024, doi: https://doi.org/10.1002/ird3.112.

[3] R. Janwadkar et al., "Focused Ultrasound for Pediatric Diseases," Pediatrics, vol. 149, no. 3, Feb. 2022, doi: https://doi.org/10.1542/peds.2021-052714.

Acknowledgments

This work has received funding from the Focused Ultrasound Foundation's Global Internship Program, the Canadian Foundation for Innovation, and the Posluns Family Foundation.